phys. stat. sol. (b) **236**, No. 2, 265–271 (2003) / **DOI** 10.1002/pssb.200301665

Application of the multicomponent Falicov–Kimball model to intermediate-valence materials: $YbInCu_4$ and $EuNi_2(Si_{1-x}Ge_x)_2$

J. K. Freericks[*,1] and **V. Zlatić**[2]

[1] Department of Physics, Georgetown University, Washington, DC 20057, USA
[2] Institute of Physics, P.O. Box 304, 10001 Zagreb, Croatia

Received 1 July 2002, accepted 15 October 2002
Published online 7 March 2003

PACS 71.28.+d, 75.10.Dg, 75.20.Hr, 75.30.Mb

We develop a formalism to solve the multicomponent Falicov–Kimball model with dynamical mean-field theory, allowing for all possible crystal-field couplings (including spin-orbit coupling). We apply these techniques to solve models of the intermediate-valence transition [as seen in $YbInCu_4$ and $EuNi_2(Si_{1-x}Ge_x)_2$] in the simple limit of no crystal field or spin-orbit coupling. We show results for the uniform spin susceptibility, the average localized electron concentration, and transport properties. We also investigate the metamagnetic transition.

Introduction and brief experimental summary The anomalous properties of intermetallic compounds like $YbInCu_4$ and $EuNi_2(Si_{1-x}Ge_x)_2$ have been the subject of many studies, because of the isostructural valence-change transition which takes place, in the absence of an external magnetic field, at a transition temperature T_v (for details see, e.g., [1, 2]). The transition is accompanied by the disappearance of the local f-moment and the low-temperature phase shows anomalies typical of a valence-fluctuating fermi liquid. The f-count is non-integral [3, 2], the conductivity is metallic with a large mean-free-path, the susceptibility is enhanced and Pauli like [1, 2], the low-temperature slope of the thermoelectric power is also enhanced [4, 6], and so is the electronic specific heat [1, 7]. The data indicate that the characteristic energy scale of the low-temperature phase is quite large and that the magnetic entropy of the rare earth ions is small. While the properties of such a fermi liquid state can be explained assuming some hybridization between the f-electrons and the conduction band, the onset of the high-entropy phase at the transition temperature T_v is difficult to explain by the Anderson or Kondo models in which the full magnetic degeneracy is not expected to emerge below the Kondo temperature $T_K \gg T_v$. We note also that the low-temperature phase of $YbInCu_4$ and $EuNi_2(Si_{1-x}Ge_x)_2$ is easily destabilized not just by temperature but by an external magnetic field as well. Applying a field larger than a critical value, $H_c(T)$, induces a metamagnetic transition and restores the f-moment [1, 2]. The thermal energy of the valence transition and the Zeeman energy of the critical field are about the same. The valence-fluctuating phase can also be destabilized by hydrostatic pressure and chemical doping.

The high-temperature phase has attracted less attention than the low-temperature one, although its features are even more surprising. It exhibits a Curie–Weiss susceptibility with a reduced Curie constant (from the nominal concentration of f-moments) and a very small Curie-Weiss temperature, as

[*] Corresponding author: e-mail: jkf@physics.georgetown.edu

 0370-1972/03/23603-0265 $ 17.50+.50/0

seen in $YbInCu_4$ and $EuNi_2(Si_{1-x}Ge_x)_2$ [1, 2]. Since $T_v \geq 50$ K in most Yb-based systems and $T_v \geq 100$ K in most Eu-based systems, the high-temperature phase is restricted to a rather narrow temperature interval in which the anomalies are not sufficiently pronounced. Their properties become most apparent if the valence-fluctuating phase is suppressed completely by pressure or doping. An interesting example is provided by $Yb_xY_{1-x}InCu_4$ in which Y-substitution above 15% stabilizes the high-temperature phase down to $T = 0$ K [4, 8] and the anomalies can be studied in a broader temperature range, and without additional features due to the transition. The experimental results for the resistivity, the thermoelectric power and the susceptibility [4] are shown in Fig. 1.

The susceptibility data show that the Curie–Weiss temperature of all samples is about the same and much less than T_v. The magnetic response of the high-temperature phase can be represented by a single universal curve, provided one scales the data by an effective concentration of magnetic f-ions, n_f, which is always smaller than the nominal concentration of f-ions. The universal shape can be explained by the crystal field (CF) theory from room temperature down to 10 K [5], which shows that the "single-ion" CF theory does capture the functional form of the susceptibility data but the "magnetic" concentration appears to be quite different from the nominal one. Below 10 K, the susceptibility deviates from the CF theory and shows an apparent reduction of the Curie constant.

The resistivity of the high-temperature phase of $Yb_xY_{1-x}InCu_4$ has a weak maximum and the thermopower has a minimum above 100 K but neither quantity shows much structure at low temperature, where the susceptibility drops below the CF values. Similar transport anomalies are also seen in $EuNi_2(Si_{1-x}Ge_x)_2$ [6], where the sign of the thermopower is reversed with respect to Yb systems. Note, the discontinuity of the thermoelectric power at the valence transition is a trivial consequence of different thermoelectric properties of the two phases: the thermopower of the valence-fluctuating

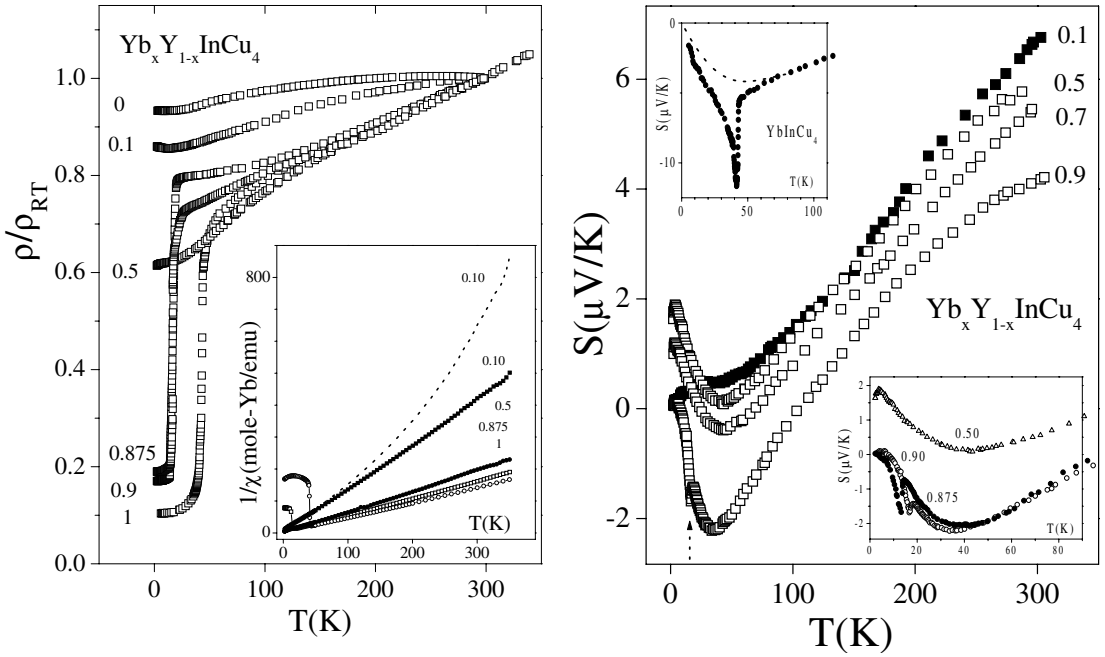

Fig. 1 The left panel shows the resistivity and the inverse magnetic susceptibility of $Yb_xY_{1-x}InCu_4$ plotted as a function of temperature for various concentrations of Y ions [4]. The dashed line shows the susceptibility of an $Yb_{0.20}Y_{0.80}InCu_4$ sample normalized to the nominal Yb concentration. Note, that all the "high-temperature" data can be collapsed onto a single universal curve (not shown here), by normalizing the susceptibility with respect to an effective Yb-concentration. The right panel shows thermopower of $Yb_xY_{1-x}InCu_4$ as a function of temperature for various concentrations of Y ions [4]. The upper inset on the left panel shows the thermopower of undoped $YbInCu_4$, and the lower inset shows the low-temperature behavior.

phase has an enhanced slope and grows rapidly up to T_v, where it drops to the values characteristic of the high-temperature phase. The experimental data indicate that the high-temperature phase is characterized by degenerate local moments which interact with the conduction band (and, hence, get reduced) but the interaction is not of the usual Kondo type because Kondo-type anomalies are not seen.

The high-temperature behavior of $YbInCu_4$- and $EuNi_2(Si_{1-x}Ge_x)_2$-like compounds can be well described by the Falicov–Kimball model [9] in which the interaction between the conduction and f-electrons is due to a Coulomb repulsion. The f-ions are allowed to exist in two configurations, which differ in their f-count by one, and the concentration of f-electrons is treated as a thermodynamical variable but the *dynamics* of the f-electrons are neglected. Here we concentrate on examining the situation where we take into account the actual degeneracy of the total angular momentum multiplet of the f-electron states. For Yb ions, the state with no f-holes has unit degeneracy, while the single-hole state has a degeneracy of 8 (corresponding to $S = 7/2$). The two-hole case is forbidden due to the mutual repulsion of two holes costing too much in energy. The crystal field of cubic symmetry lifts the 8-fold degeneracy of a single f-hole in $YbInCu_4$-like systems, and gives rise to 2 doublets and a quartet, unless there is some accidental degeneracy. For Eu ions in $EuNi_2(Si_{1-x}Ge_x)_2$-like systems, we consider only two ionic configurations: the one corresponding to Eu $4f^6$ (3^+), with a non-magnetic ground state and two excited magnetic states, and the other one describing the magnetic $4f^7$ (2^+) state of Eu ions. All other states of the Eu ions are higher in energy and are neglected. The crystal field of tetragonal symmetry splits the 8-fold degenerate magnetic f-state into 4 doublets, while the magnetic field gives rise to Zeeman splittings. For simplicity, we discuss the case of Yb ions and consider the Zeeman splitting only. The generalization to the CF-split case or to Eu ions is straightforward and will appear elsewhere.

Theoretical formalism The Falicov–Kimball model is the simplest model of correlated electrons. The original version [9] involved spin-one-half-electrons. Here, we generalize to the case of an arbitrary degeneracy of the $(2s+1)$ itinerant and $(2S+1)$ localized electrons. The Hamiltonian is then

$$\mathcal{H} = -t \sum_{\langle ij \rangle} \sum_{\sigma=1}^{2s+1} c_{i\sigma}^{\dagger} c_{j\sigma} + \sum_{i} \sum_{\eta=1}^{2S+1} E_{f\eta} f_{i\eta}^{\dagger} f_{i\eta} + U \sum_{i} \sum_{\sigma=1}^{2s+1} \sum_{\eta=1}^{2S+1} c_{i\sigma}^{\dagger} c_{i\sigma} f_{i\eta}^{\dagger} f_{i\eta}$$
$$- g\mu_B H \sum_{i} \sum_{\sigma=1}^{2s+1} m_\sigma c_{i\sigma}^{\dagger} c_{i\sigma} - g_f \mu_B H \sum_{i} \sum_{\eta=1}^{2S+1} m_\eta f_{i\eta}^{\dagger} f_{i\eta} \,. \tag{1}$$

The symbols $c_{i\sigma}^{\dagger}$ ($c_{i\sigma}$) denote the itinerant electron creation (annihilation) operators at site i in state σ (the index σ takes $2s+1$ values). Similarly, the symbols $f_{i\eta}^{\dagger}$ ($f_{i\eta}$) denote the localized electron creation (annihilation) operators at site i in state η (the index η takes $2S+1$ values). We identify the index σ and η with the z-component of total angular momentum. The first term is the kinetic energy (hopping) of the conduction electrons (with $t = t^*/2\sqrt{d}$ denoting the nearest-neighbor hopping integral and all energies measured in units of t^*); the summation is over nearest neighbor sites i and j (we count each pair twice to guarantee hermiticity). The second term is the localized electron site energy (which we allow to depend on the index η to include crystal-field effects). The third term is the Falicov–Kimball interaction term (of strength U) which represents the local Coulomb interaction when itinerant and localized electrons occupy the same lattice site. Finally, the fourth and fifth terms represent the interaction with an external magnetic field H, with μ_B the Bohr magneton, g (g_f) the respective Landé g-factors, and m_σ (m_η) the z-component of total angular momentum for the respective states (in this formulation we are assuming that J_z commutes with the crystal-field Hamiltonian so the crystal-field and magnetic terms are simultaneously diagonalizable; this assumption is not necessary, but it does simplify the notation). The chemical potential μ is employed to adjust the total electron concentration. We restrict ourselves to the case where the f–f interaction energy is infinite, so there is no more than one localized electron per site.

In the large-dimensional limit, the self energy for the Falicov–Kimball model $\Sigma_\sigma(z)$ becomes local [10], so the local Green's function can be expressed as an integral over the noninteracting density of states

(DOS) $\rho(\epsilon) = \exp(-\epsilon^2)/\sqrt{\pi}$ (for the hypercubic lattice)

$$G_\sigma(z) = \int \mathrm{d}\epsilon\, \rho(\epsilon)\, \frac{1}{z + \mu + g\mu_B H m_\sigma - \Sigma_\sigma(z) - \epsilon} \tag{2}$$

with z in the complex plane. The local self energy is found by solving the impurity problem in the presence of a time dependent field $\lambda_\sigma(\tau,\tau') = \lambda_\sigma(\tau - \tau')$. This proceeds in a number of steps [11]. First we determine the partition function of a generalized impurity via

$$\mathcal{Z}_{\mathrm{imp}}(\lambda) = \mathrm{Tr}_{cf}[\mathcal{T}_\tau\, \mathrm{e}^{-\beta\mathcal{H}_{\mathrm{imp}}}\, S(\lambda)]\,, \tag{3}$$

with $\mathcal{H}_{\mathrm{imp}}$ the impurity Hamiltonian which can be written in the most general form as

$$\mathcal{H}_{\mathrm{imp}} = -\sum_{\sigma=1}^{2s+1} (\mu + g\mu_B H m_\sigma)\, c_\sigma^\dagger c_\sigma + \mathcal{H}_f + U \sum_{\sigma=1}^{2s+1} \sum_{\eta=1}^{2S+1} c_\sigma^\dagger c_\sigma f_\eta^\dagger f_\eta\,, \tag{4}$$

where we have kept the f Hamiltonian to be as general as possible (allowing all crystal-field and spin–orbit terms; in the case we treat here, there are no spin–orbit terms considered but we can be fully general in the formalism), and

$$S(\lambda) = \mathcal{T}_\tau\, \mathrm{e}^{-\int_0^\beta \mathrm{d}\tau \int_0^\beta \mathrm{d}\tau'\, \Sigma_\sigma \lambda_\sigma(\tau-\tau')\, c_\sigma^\dagger(\tau)\, c_\sigma(\tau')}\,. \tag{5}$$

The operator $c_\sigma(\tau) = \exp(\tau\mathcal{H}_{\mathrm{imp}})\, c_\sigma(0) \exp(-\tau\mathcal{H}_{\mathrm{imp}})$.

The dynamics of the f-electron are trivial, since the f-number operator commutes with the impurity Hamiltonian and the trace over f states can be separated into a sum over the states with a fixed number of f-particles. In the case of Yb, we consider the state with zero f-holes and with one f-hole and the end result becomes

$$\mathcal{Z}_{\mathrm{imp}} = \mathcal{Z}_0(\lambda,\mu) + \mathcal{Z}_0(\lambda,\mu - U)\mathcal{Z}_1^f \tag{6}$$

with

$$\mathcal{Z}_0(\lambda,\mu) = \prod_{\sigma=1}^{2s+1} \left[2\, \mathrm{e}^{-\beta(\mu + g\mu_B H m_\sigma)/2} \prod_{n=-\infty}^{\infty} \frac{i\omega_n + \mu + g\mu_B H m_\sigma - \lambda_\sigma(i\omega_n)}{i\omega_n + \mu + g\mu_B H m_\sigma}\right] \tag{7}$$

where $i\omega_n = i\pi T(2n+1)$ is the fermionic Matsubara frequency and $\lambda_\sigma(i\omega_n)$ is the Fourier transform of $\lambda_\sigma(\tau - \tau')$ and

$$\mathcal{Z}_1^f = \mathrm{Tr}_{f\,:\,n_f=1}\, \mathrm{e}^{-\beta\mathcal{H}_f} = \sum_{\eta=1}^{2S+1} \mathrm{e}^{-\beta(E_{f\eta} - g\mu_B H m_\eta)}\,. \tag{8}$$

In the case of Eu ions the invariant f-subspace is defined by the constraint $n_f = 6$ and $n_f = 7$, respectively. That is, the two configurations differ by one f-electron and the only change with respect to the Yb case discussed above is that the partition function becomes,

$$\mathcal{Z}_{\mathrm{imp}} = \mathcal{Z}_0(\lambda,\mu)\, \mathcal{Z}_6^f + \mathcal{Z}_0(\lambda,\mu - U)\, \mathcal{Z}_7^f \tag{9}$$

where $\mathcal{Z}_7^f$ is the same as $\mathcal{Z}_1^f$ and

$$\mathcal{Z}_6^f = \mathrm{Tr}_{f\,:\,n_f=6}\, \mathrm{e}^{-\beta\mathcal{H}_f} = \mathrm{e}^{-\beta E_{6\eta}} + \sum_{\eta=1}^{2} \mathrm{e}^{-\beta(E'_{6\eta} - g'_f \mu_B H m_\eta)}\,. \tag{10}$$

The g-factors are different for the six and seven electron states, and $E'_{6\eta}$ is the crystal-field split energy of the excited magnetic state with six electrons.

Second, we determine the impurity Green's function by $G_\sigma(i\omega_n) = -d \ln \mathcal{Z}_{\mathrm{imp}}/\mathrm{d}\lambda_\sigma(i\omega_n)$ which becomes

$$G_\sigma(i\omega_n) = \frac{w_0}{i\omega_n + \mu + g\mu_B H m_\sigma - \lambda_\sigma(i\omega_n)} + \frac{w_1}{i\omega_n + \mu + g\mu_B H m_\sigma - \lambda_\sigma(i\omega_n) - U}\,. \tag{11}$$

Third, the self energy is found from

$$\Sigma_\sigma(i\omega_n) = i\omega_n + \mu + g\mu_B H m_\sigma - \lambda_\sigma(i\omega_n) - G_\sigma^{-1}(i\omega_n)\,. \tag{12}$$

Here we have $w_1 = 1 - w_0$ and

$$w_0 = \mathcal{Z}_0(\lambda,\mu)/\mathcal{Z}_{\rm imp}\,; \tag{13}$$

note that w_1 is equal to the average f-electron concentration n_f.

The Green's function is determined by the following algorithm [12]: (i) we start with $\Sigma = 0$; (ii) use Eq. (2) to determine the local Green's function; (iii) employ Eq. (12) to find the dynamical mean field λ; (iv) calculate w_0 from Eq. (13) and the impurity Green's function from Eq. (11); and (v) use Eq. (12) to find the new self energy. This is repeated until the Green's function converges.

Once the Green's function is determined on the imaginary axis, one can iterate the analytic continuation of these equations (with w_0 fixed) and calculate the Green's functions on the real axis. Then one can determine the transport by evaluating the bare bubble for the dc conductivity [13] and then use the Jonson-Mahan theorem for the thermal transport [14–16]. The result for the dc conductivity is

$$\sigma_{dc} = \sigma_0 \int_{-\infty}^{\infty} {\rm d}\omega \left(-\frac{{\rm d}f(\omega)}{{\rm d}\omega}\right) \sum_{\sigma=1}^{2s+1} \tau_\sigma(\omega)\,, \tag{14}$$

with the spin-dependent relaxation time equal to

$$\tau_\sigma(\omega) = \frac{{\rm Im}\, G_\sigma(\omega)}{{\rm Im}\, \Sigma_\sigma(\omega)} + 2 - 2\,{\rm Re}\,\{[\omega + \mu + g\mu_B H m_\sigma - \Sigma_\sigma(\omega)]\, G_\sigma(\omega)\}\,. \tag{15}$$

The thermal transport (such as the thermopower S and the electronic contribution to the thermal conductivity κ_e) are expressed in terms of three different transport coefficients $L_{11}, L_{12} = L_{21}$ and L_{22} as follows:

$$\sigma_{dc} = e^2 L_{11}\,, \qquad S = \frac{k_B}{|e|T}\frac{L_{12}}{L_{11}}\,, \qquad \kappa_e = \frac{k_B^2}{T}\left[L_{22} - \frac{L_{12}L_{21}}{L_{22}}\right], \tag{16}$$

with k_B the Boltzmann constant. The individual transport coefficients are determined by the zero-frequency limit of the analytic continuation of the relevant polarization operators $L_{ij} = \lim_{\nu\to 0} {\rm Re}\,[i\bar{L}_{ij}(\nu)/\nu]$ with

$$\bar{L}_{11}(i\nu_l) = \int_0^\beta {\rm d}\tau\, {\rm e}^{i\nu_l\tau}\, {\rm Tr}_{cf}\, \frac{\langle \mathcal{T}_\tau\, {\rm e}^{-\beta\mathcal{H}}\, j_n(\tau)\, j_n(0)\rangle}{\mathcal{Z}_L}\,, \tag{17}$$

$$\bar{L}_{12}(i\nu_l) = \int_0^\beta {\rm d}\tau\, {\rm e}^{i\nu_l\tau}\, {\rm Tr}_{cf}\, \frac{\langle \mathcal{T}_\tau\, {\rm e}^{-\beta\mathcal{H}}\, j_n(\tau)\, j_Q(0)\rangle}{\mathcal{Z}_L}\,, \tag{18}$$

and

$$\bar{L}_{22}(i\nu_l) = \int_0^\beta {\rm d}\tau\, {\rm e}^{i\nu_l\tau}\, {\rm Tr}_{cf}\, \frac{\langle \mathcal{T}_\tau\, {\rm e}^{-\beta\mathcal{H}}\, j_Q(\tau)\, j_Q(0)\rangle}{\mathcal{Z}_L}\,, \tag{19}$$

where the subscripts n and Q denote the number (charge) and heat currents respectively (and we suppressed the Cartesian vector indices); $\mathcal{Z}_L$ is the partition function for the lattice. All of these correlation functions are determined by their corresponding bare bubbles, because there are no vertex corrections for any of them. There is a simple relation between these different transport coefficients

$$\frac{e^2}{\sigma_0}\, L_{ij} = \int_{-\infty}^{\infty} {\rm d}\omega \left(-\frac{{\rm d}f(\omega)}{{\rm d}\omega}\right) \sum_{\sigma=1}^{2s+1} \tau_\sigma(\omega)\, \omega^{i+j-2}\,, \tag{20}$$

which allows the thermal transport to be determined.

Metamagnetism can be calculated by examining the solutions in a magnetic field. The average magnetization is

$$\langle m_f \rangle = \frac{\mathcal{Z}_0(\lambda, \mu - U)}{\mathcal{Z}_{\rm imp}} \sum_{\eta=1}^{2S+1} m_\eta \, {\rm e}^{-\beta(E_{f\eta} - g\mu_B H m_\eta)} = \langle n_f \rangle \, \frac{1}{\mathcal{Z}_f} \sum_{\eta=1}^{2S+1} m_\eta \, {\rm e}^{-\beta(E_{f\eta} - g\mu_B H m_\eta)} , \tag{21}$$

which is the expected "crystal-field" result, reduced by the average f-filling $0 \leq \langle n_f \rangle \leq 1$. Because of this reduction, the temperature-dependent Curie constant is reduced by the same factor.

Theoretical result The main result we wish to show here is the effect of increasing the localized electron degeneracy on the phase transition of the Falicov–Kimball model. We choose the f-level E_f to be the same for all η states, and equal to -0.6 (i.e., no CF splitting). The renormalized f-level lies above the chemical potential at $T = 0$, so there are no f-electrons in the ground state, but it is tuned to lie close to the chemical potential, so as T increases, the f-occupancy increases, producing a local-moment response. Since the filling of the f electrons is entropically driven, we expect the filling to increase rapidly with T as the degeneracy increases. In Fig. 2, we plot the average f-occupation and the spin susceptibility (normalized by the average of m_z^2 which equals 1/2 for spin-one-half and 42 for spin-seven-halves) for two cases: spin 1/2 and spin 7/2. We pick two values of U, a weaker correlated system at $U = 2$ and a stronger correlated one at $U = 4$. The total electron filling is 1.5. The solid lines are for $U = 2$ and the dotted for $U = 4$, while the thin lines are $S = 1/2$ and the thick lines are $S = 7/2$.

One can see in panel (a) that as the degeneracy increases from two to eight, the high temperature value of n_f increases, the "transition temperature" decreases, and the transition becomes sharper (at even higher temperatures n_f increases even more in the degenerate case). Increasing U to 4 broadens the overall transition, but the qualitative effects of adding f-states is the same. In panel (b), we plot the spin susceptibility, which satisfies a Curie-like form, but with a temperature dependent concentration of local f-moments. Hence it has a peaked form, with a sharp reduction of the magnetic response as $T \to 0$. Once again, the susceptibility is enhanced, sharpened, and T_v moves to lower temperature as the degeneracy increases. Increasing U (for fixed E_f) broadens the transition.

We can also investigate the transport properties of these solutions. Here we see some interesting results, as shown in Fig. 3. In panel (a), we see that the resistivity has a maximum at an effective temperature T^* which is much larger than T_v. This occurs due to the development of a gap in the single-particle DOS at high temperature driven by the increased f-electron occupation and the Falicov–Kimball interaction. The peak sharpens and is significantly enhanced as the degeneracy increases; experiment does not show this large enhancement, rather the resistivity is rather flat. Increasing U pushes T^* to higher energies. The results are somewhat similar for the thermopower in panel (b), except here we see the peaks sharpening for higher degeneracy, although the maximal value of S does not change substantially with degeneracy. The location of the peak in the thermopower is pushed to a lower temperature though.

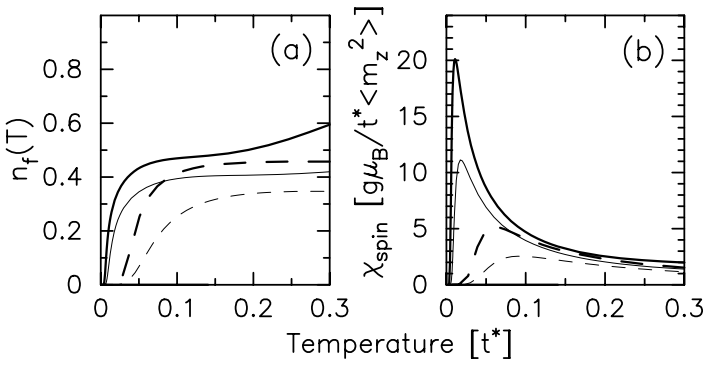

Fig. 2 (a) Localized electron filling and (b) normalized spin susceptibility for the Falicov–Kimball model with $n_{\rm tot} = 1.5$ and $E_f = -0.6$. The solid lines are for $U = 2$ and the dashed lines are for $U = 4$. The thick lines are for an eightfold degenerate case ($S = 7/2$), and the thin lines are for a twofold degeneracy ($S = 1/2$).

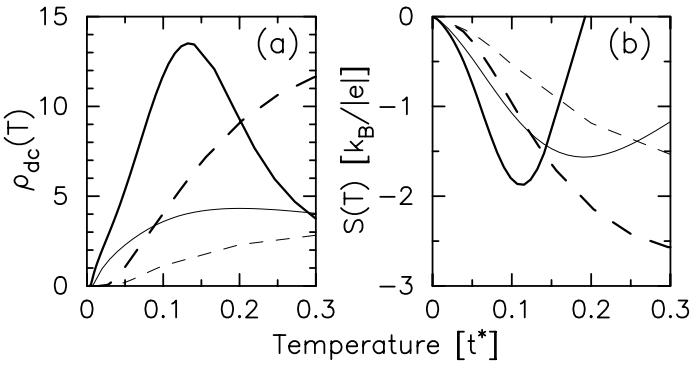

Fig. 3 (a) DC resistivity and (b) thermopower for the Falicov–Kimball model with $n_{tot} = 1.5$ and $E_f = -0.6$. The solid lines are for $U = 2$ and the dashed lines are for $U = 4$. The thick lines are for an eightfold degenerate case, and the thin lines are for a twofold degeneracy.

Conclusions We developed the formalism to describe the Falicov–Kimball model with arbitrary crystal-field and spin-orbit couplings for the localized electrons. These generalizations are needed to explain a number of the anomalous features seen in the high-temperature phase of valence-change materials like $YbInCu_4$ and $EuNi_2(Si_{1-x}Ge_x)$. We numerically analyzed the simplified case of considering the proper degeneracy for the Yb ions, and saw that it produced a number of interesting features: (i) the valence-change transition was sharpened and the total magnitude of the valence change increased and (ii) the peak in the resistivity was enhanced and moved to lower temperature, while the peak for the thermopower was only slightly enhanced, but also moved to lower temperature. We plan to further investigate these systems, including more complicated crystal-field and spin-orbit couplings, elsewhere.

Acknowledgement This research was suported by the N.S.F. under grant number DMR 9973225.

References

[1] J. L. Sarrao, Physica B, **259 & 261**, 129 (1999).
[2] H. Wada, A. Nakamura, A. Mitsuda, M. Shiga, T. Tanaka, H. Mitamura, and T. Goto, J. Phys.: Condens. Matter **9**, 7913 (1997).
[3] C. Dallera, M. Grioni, A. Shukla, G. Vankó, J. L. Sarrao, J. P. Rueff, and D. L. Cox, Phys. Rev. Lett. **88**, 196403 (2002).
[4] M. Ocko and J. Sarrao, Physica B **312/313**, 341 (2002).
[5] I. Aviani et al., unpublished.
[6] J. Sakurai, S. Fukuda, A. Mitsuda, H. Wada and M. Shiga, Physica B **281/282**, 134 (2000).
[7] H. Wada, H. Gomi, A. Mitsuda, and M. Shiga, Solid State Commun. **117**, 703 (2001).
[8] A. Mitsuda, T. Goto, K. Yoshimura, W. Zhang, N. Sato, K. Kosuge, and H. Wada, Phys. Rev. Lett. **88**, 137204 (2002).
[9] L. M. Falicov and J. C. Kimball, Phys. Rev. Lett. **22**, 997 (1969).
[10] U. Brandt and C. Mielsch, Z. Phys. B **75**, 365 (1989).
[11] V. Zlatić, J. K. Freericks, R. Lemański, and G. Czycholl, Philos. Mag. B **81**, 1443 (2001).
[12] M. Jarrell, Phys. Rev. Lett. **69**, 168 (1992).
[13] A. Khurana, Phys. Rev. Lett. **64**, 1990 (1990).
[14] M. Jonson and G. D. Mahan, Phys. Rev. B **21**, 4223 (1980).
[15] M. Jonson and G. D. Mahan, Phys. Rev. B **42**, 9350 (1990).
[16] J. K. Freericks and V. Zlatić, Phys. Rev. B **64**, 073109 (2001); Erratum: Phys. Rev. B **66**, 249901 (2002).